Pflügers Arch - Eur J Physiol (2002) 443:418–426
DOI 10.1007/s004240100690

ORIGINAL ARTICLE

Martin Heine · Evgeni Ponimaskin · Ulf Bickmeyer
Diethelm W. Richter

5-HT-receptor-induced changes of the intracellular cAMP level monitored by a hyperpolarization-activated cation channel

Received: 1 June 2001 / Revised: 12 July 2001 / Accepted: 12 July 2001 / Published online: 22 September 2001

Abstract The HvCNG channel from the moth *Heliothis virescens* is highly sensitive to cAMP concentrations ranging between 0.1 µM and 5 µM. This HvCNG channel was over-expressed in *Spodoptera frugiperda* (Sf.9) cells to measure endogenous cAMP levels. Hyperpolarization-activated inward currents were measured in the whole-cell patch-clamp configuration with pipettes filled with different cAMP concentrations to calibrate the system. Varying the cAMP concentration between 0 µM and 100 µM in the pipette, the half-maximal activation voltage ($V_{1/2}$) was shifted by +28.5±1.7 mV. The activation time constant (τ_a) was used as a parameter for cAMP quantification because it was independent of the expression level of HvCNG channels. τ_a changed from 1106±60 ms at 0 µM cAMP to 265±7 ms at a saturating concentration of 1 mM cAMP. A dose–response relationship yielded values of 0.6 µM for the half-maximal cAMP concentration and 1.5 for the Hill coefficient. Activation of endogenous adenylyl cyclases by 50 µM forskolin induced an elevation of the cAMP level by about 1.6±0.2 µM. Co-expressions of HvCNG channels in combination with the mouse 5-$HT_{4(a)}$- or 5-HT_{1A}- receptors and the corresponding G_s- or G_i-proteins were successful and allowed us to also verify receptor-induced changes of the cAMP level. Stimulation of m5-$HT_{4(a)}$-receptors by 0.1 µM 5-HT induced an increase of cAMP of about 4.6±1.5 µM, whereas cAMP levels decreased from a control value of 1±0.2 µM to 0.41±0.1 µM after stimulation of the m5-HT_{1A}-receptors.

Keywords cAMP measurement · Hyperpolarization-activated cation (HCN) channels · G-proteins · Signal transduction

M. Heine · E. Ponimaskin · U. Bickmeyer · D.W. Richter (✉)
Institute of Physiology and Pathophysiology,
Department of Neuro- and Sensory Physiology Humboldtallee 23,
Georg-August-University Göttingen, Germany
e-mail: drichte@popper.gwdg.de
Tel.: +49-551-395911, Fax: +49-551-396031

Introduction

The second messenger cAMP has indirect effects on many processes, but one of its direct functions is to modulate the opening kinetics of certain ion channels. Two closely related families of such ion channels are the cyclic-nucleotide-gated cation channels (CNG) (for review [10, 33]) and the hyperpolarization-activated cation channels (HCN) that generate the hyperpolarization-activated cation currents I_h, I_f or I_Q (for review [21, 27]). The open probability of both types of ion channels and their opening kinetics change in relation to the cGMP and cAMP concentrations [8, 10, 24]. The molecular structure that is responsible for such behaviour is the cyclic-nucleotide-binding domain (CNBD) on the C-terminal of each of the four channel subunits. In both channel types the CNBDs are similar in their amino acid sequence, but HCN channels are about 10- to 1000-fold more sensitive to cAMP than CNG channels [10, 27, 35].

The intracellular cAMP level depends mainly on the activity of two enzymes, the adenylyl cyclases (AC) catalysing cAMP production and the phosphodiesterases (PDE) degrading the cAMP. Guanine-nucleotide-binding proteins (G-proteins) activated by certain metabotropic receptors are physiological regulators of the AC's [12, 19] and are known to modulate HCN channels (I_h) through intracellular cAMP [5, 11, 22]. These established functions encouraged us to use a HCN channel as a cellular biosensor for monitoring regulatory changes in cAMP concentrations.

We used the baculovirus expression system in Sf.9 cells, in which HCN channels were co-expressed with a serotonin (5-HT) receptor and G-proteins from mouse. The specific HCN channel type used in the present study was cloned from an antennal cDNA library of the moth *Heliothis virescens*, which represents a cyclic-nucleotide- and voltage-activated cation channel (HvCNG) belonging to the HCN gene family [14]. The m5-$HT_{4(a)}$-receptor isoform is described to activate ACs via a G_s-protein [3, 9], while the m5-HT_{1A}-receptor is known to reduce the intracellular cAMP level via a G_i-protein, espe-

cially due to its coupling to the α_i-subunit [3]. However, the m5-HT_{1A}-receptor can also elevate the cAMP level through the β/γ-subunits [2, 16] that activate ACs.

In order to calibrate the endogenous sensitivity of HvCNG channels, we analysed the activation kinetics of the HvCNG current to gain a quantitative parameter for determining intrinsic cAMP levels. The experiments proved that the system is valid for obtaining information about the coupling efficacy between receptor and G-protein subunits.

Materials and methods

Construction of recombinant baculovirus

All basic DNA procedures were performed as described elsewhere [26]. Dr. Aline Dumuis (Montpellier; France) kindly provided us with the m5-$HT_{4(a)}$ gene. The m5-$HT_{4(a)}$ cDNA was cleaved with *Xba*I and *Hin*dIII endonucleases to yield the 1.1-kb fragment containing the entire coding sequence. The fragment was ligated to the *Xba*I and *Hin*dIII sites in the multiple cloning site of the pFastBac donor plasmid (Life Technologies; Eggenstein-Leopoldshaven, Germany). The cDNA encoding for the m5-HT_{1A}-receptor was kindly provided by Dr. Paul Albert (Montreal, Canada). The m5-HT_{1A} gene was cut out from pBlueScript plasmid with *Eco*RI and then ligated into *Eco*RI site in MCS of pFastBac vector. The final plasmids were transfected into the DH10Bac *E. coli* cells containing bacmid and helper DNA. Recombinant bacmid DNA was purified, checked for the existence of m5-HT_{1A} or m5-$HT_{4(a)}$ genes by PCR with receptor-specific primers and then transfected into *Spodoptera frugiperda* (Sf.9) cells by the Cellfectin reagent (Life Technologies; Eggenstein-Leopoldshaven, Germany). Finally, the recombinant viruses were purified and amplified as described previously [32].

Expression of recombinant proteins in Sf.9 cells

The recombinant HvCNG/AcNMPV baculovirus was a gift from Professor H. Breer (Stuttgart) [14]. For expression of HvCNG channels, Sf.9 cells (1.5×10^6) grown in TC 100 medium (Life Technologies; Eggenstein-Leopoldshaven, Germany) supplemented with 10% fetal calf serum (FCS) and 1% penicillin/streptomycin in 35-mm dishes were infected with recombinant baculovirus at multiplicity of infections (m.o.i.) of 10. For the co-expression experiments, Sf.9 cells were infected with HvCNG channels and also with recombinant baculoviruses encoding for the m5-$HT_{4(a)}$-receptor or the m5-HT_{1A}-receptor, the α_s- or the α_i-subunit as well as β_1/γ_2-subunits of trimeric G-proteins beside the HvCNG channel at a m.o.i. of at least 1 for each type of virus. After 48 h post-infection Sf.9 cells were used for electrophysiological or Western blot analysis.

SDS-PAGE and Western blotting

Sf.9 cells expressing m5-$HT_{4(a)}$-receptors, HvCNG channels, $G\alpha_s$-, $G\beta_1$- and $G\gamma_2$-subunits were scraped into medium 48 h post-infection and washed in ice-cold PBS (140 mM NaCl, 3 mM KCl, 2 mM KH_2PO_4, 6 mM Na_2HPO_4, pH 7.4). Cells were than resuspended in Tris/EDTA buffer (10 mM Tris/HCl, pH 8.0, 1 mM EDTA) and boiled for 3 min in non-reducing electrophoresis sample buffer (62.5 mM Tris-HCl, pH 6.8, containing 20% glycerol, 6% SDS, 0.002% bromphenol blue). Proteins were separated by SDS-PAGE on 10% acrylamide gels using standard procedures. After the SDS-PAGE was completed, the proteins were blotted to a PVDF transfer membrane (Hybond-P; Amersham, Germany) using a semi-dry blotter at 5 mA per cm^2. Membranes were probed for m5-$HT_{4(a)}$-receptors with antibodies AS9459 raised against the C-terminal peptide of m5-$HT_{4(a)}$ [23] at a 1:1000 dilution. For $G\beta_1$ and $G\gamma_2$ we used antibodies AS398 against β-subunits (β_1+β_4) and AS292 against the γ-subunits (γ_2+γ_3) at a dilution of 1:500 [15]. m5-HT_{1A}-receptors and $G\alpha_s$-subunits were detected by using anti-m5-HT_{1A}-receptor and anti-$G\alpha_s$ rabbit polyclonal antibodies at a dilution of 1:500 (Santa Cruz; Heidelberg, Germany). Detection was achieved with the enhanced chemiluminescence kit (ECL Plus; Amersham, UK). Protein bands were visualized by fluorography using Kodak X-Omat AR films and film exposure times ranging between 10 s and 60 min.

Electrophysiology

HvCNG currents were recorded in the whole-cell patch-clamp mode. Borosilicate glass pipettes were fire polished and had a resistance of 4–8 MΩ. We used the discontinuous single-electrode voltage-clamp amplifier SEC-05L from npi-electronic (Tamm, Germany), which was connected with an ITC-16 interface from Instrutech (Greatneck, N.Y., USA). Data were acquired with a computer, stored by Pulse-PulseFit 8.31 software from HEKA (Lambrecht, Germany) and analysed with Igor-WaveMetrics software (Oregon, USA).

The measurements were performed using TC 100 medium (Life Technologies; Eggenstein-Leopoldshaven, Germany) without FCS. In this medium it was possible to keep cells intact for 4–7 h. The temperature of the bath solution was held at 25±0.2°C with a Peltier-element-gated control unit from ESF-electronic (Goettingen, Germany).

The standard pipette solution contained (in millimolar concentrations): 110 K-gluconate, 1 $CaCl_2$, 2 $MgCl_2$, 2 Na_2ATP, 0.4 GTP, 10 HEPES, 10 EGTA and was adjusted to pH 7.25 with KOH shortly before use. The high gluconate concentration of the intracellular solution resulted in a liquid junction potential (measured according to [20]) of –4 mV, which was subtracted from potentials in Fig. 1, 2 and 4. The highly Ca^{2+}-buffered (10 mM EGTA) pipette solution containing 15.3 nM free Ca^{2+} concentration ("patcher power tools" software written by Francisco Mendez, Göttingen) was used, because the possible role of Ca^{2+} ions in the modulation of channel activation kinetics remains controversial [4, 18]. In some experiments, Na-cAMP was added in varying concentrations to the pipette solution to calibrate the changes of current kinetics in response to different cAMP concentrations. The osmolarity of the pipette solution was adjusted to 20 mosmol below the osmolarity of TC 100 medium. Endogenous AC were activated by 50–100 µM forskolin and blocked by 30 µM MDL 12–330A, while the m5-HT_{4a}-receptor and m5-HT_{1A}-receptor were stimulated with 0.1–50 µM serotonin (5-HT).

Drugs were applied to individual cells by pressure application (PDES 2L-unit from npi-electronic, Tamm, Germany) through pipettes (diameter of 3–5 µm) or applied to the bath solution. All chemicals were purchased from Sigma Aldrich (Germany), Merck (Darmstadt, Germany), Tocris (Bristol, UK) and Calbiochem (Bad Soden, Germany).

Data fitting

Leakage currents were automatically subtracted from the original recordings before analysis by a P/4 protocol. Two types of fittings were performed: an exponential fit of the time course of channel activation and a Boltzmann fit of the steady-state activation of tail currents. The activation time constants were fitted by the equation $I(t)=I_0+I_1\cdot[1-\exp(-t/\tau)]$, where I_0 is the current at the beginning of activation and I_1 is the maximal current at the end of the applied voltage pulses. The exponent $-t/\tau$ represents the ratio between the time t and the activation time constant τ. The fits were performed for all data points collected between the minima of the first time derivative of the current and the maximal current amplitude at the end of the voltage pulse (Fig. 1B). For the Boltzmann fit of the steady-state activation curve of HvCNG current we used equation

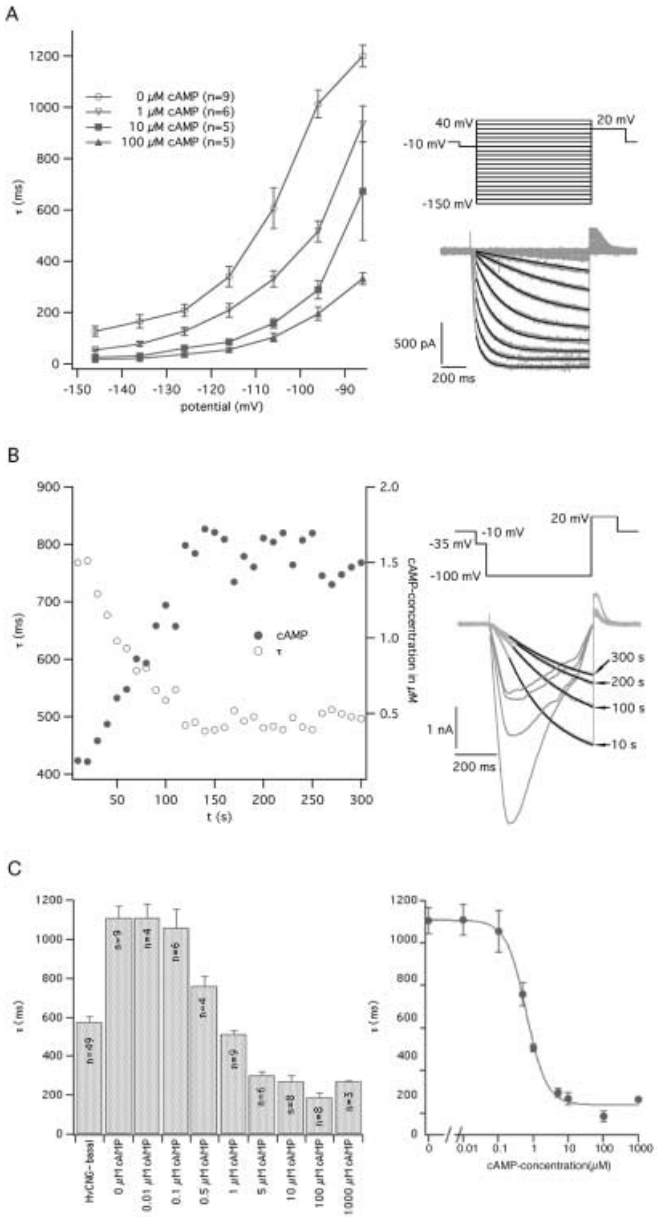

Fig. 1A–C Activation kinetic of the HvCNG channel with different free cAMP concentrations in the pipette solution (whole cell). **A** Activation constants were yielded from exponential fits of currents at voltage pulses between –150 and –90 mV (*left*). Voltage protocol and elicited currents (*right*) are shown. **B** The determination of time constants induced by 0.5 µM cAMP in the pipette solution indicates the time course of the equilibration of the intracellular milieu with the pipette solution after establishing the whole-cell configuration. Each *point* represents the activation time constant (τ_a) of a 1-s-long pulse to –100 mV (*left*). Values were revealed from single exponential fits at different times as shown for four current traces. To have a defined start and end point, currents were fitted from the minimum of the first time derivative to the end of the pulse as seen in the example (*right*). **C** τ_a shown for different cAMP concentrations (mean ±SEM). τ_a was determined for hyperpolarizing steps from the holding potential to –100 mV. The data indicate a half-maximal activation at 0.62 µM cAMP and a Hill coefficient of 1.51

$P_\infty(V_m)=1/\{1+\exp[(V_m-V_h)/k]\}$, where $P_\infty(V_m)$ denotes the steady-state open probability P_∞ of HvCNG channels at a membrane potential V_m, V_h is the half-activation voltage of the HvCNG current, and k is the slope factor. cAMP levels were calculated from the dose–response relationship shown in Fig. 1C. Data for the dose–response curve were fitted by a Hill equation with variable slope $\tau_{min}+(\tau_{max}-\tau_{min})/1+(c_{1/2}/c)^n$, where τ_{min} is the time constant at 0 cAMP, τ_{max} is the time constant at 1 mM cAMP, $c_{1/2}$ is the half-maximal cAMP concentration and n is the Hill factor. To calculate the cAMP concentration for each time constant between τ_{min} and τ_{max} we converted the Hill equation to:

$$c = (\tau-\tau_{min})/(\tau_{max}-\tau_{min})\cdot c_{1/2}^{n}/\left\{1-[(\tau-\tau_{min})/(\tau_{max}-\tau_{min})]^{(1/n)}\right\}$$

Statistical values are given as means ±SEM.

Results

Sf.9 cells are spherical cells with a diameter ranging between 10 µm and 15 µm. Activation of the recombinant m5-$HT_{4(a)}$-/m5-HT_{1A}-receptor-controlled second messenger cascade was functional in these cells and the stimulation of intracellular ACs by forskolin was partially reversible. This suggests that wash-out effects did not affect the cAMP-induced changes in channel kinetics. This enabled us to measure intracellular concentrations of cAMP with a technique relying on patch-clamp recordings.

Estimation of cAMP levels

The absolute current amplitudes varied largely between individual cells depending on the expression level of HvCNG channels in Sf.9 cells. The maximal currents varied between 0.1 nA and 2.5 nA when –100-mV pulses lasting for 1 s were applied.

In order to be independent of the expression levels of HvCNG channels, we measured two kinetic parameters: the half-maximal activation voltage ($V_{1/2}$) and the voltage-dependent activation time constant (τ_a) near $V_{1/2}$ (–100 mV; Figs. 1A, C, 2). A dose–response curve of cAMP concentrations was determined by loading cells with various concentrations of Na-cAMP added to the pipette solution. The current activation by hyperpolarizing pulses stepping from –10 mV to –100 mV was well fitted by a single exponential curve. The τ_a value was cAMP dependent and changed from 1106±60 ms at 0 µM cAMP (n=9) to 265±7 ms at 1 mM cAMP (n=3) (Fig. 1C). In the presence of 30 µM MDL 12330A, a blocker of ACs [13], the τ_a value for 0 cAMP was not significantly different, namely 1115±86 ms (n=8).

Measurements were not started for at least 5 min after establishing the whole-cell configuration, so as to allow equilibration of the cAMP concentrations between the pipette solution and the cytosol (Fig. 1B). The activation curve as determined by tail currents was fitted by the Boltzmann equation and showed a pronounced voltage

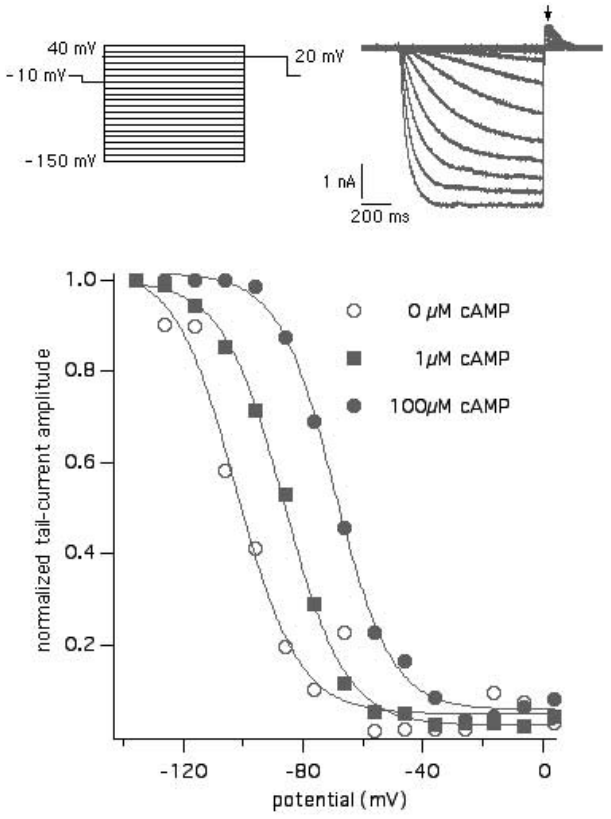

Fig. 2 Tail current analysis for three different cAMP concentrations. Tail currents were measured at the time indicated by the *arrow*. Normalized tail current amplitudes were fitted by a Boltzmann equation. The fitting values are $V_{1/2}$=–102.9±2.03 mV, slope = 11.3±0.82 for 0 cAMP (n=8), $V_{1/2}$=–90.6±2.82 mV, slope = 12.2±1.6 for 1 μM cAMP (n=4), $V_{1/2}$=–74.5±1.71 mV, slope = 8.85±1.9 for 100 μM cAMP (n=3)

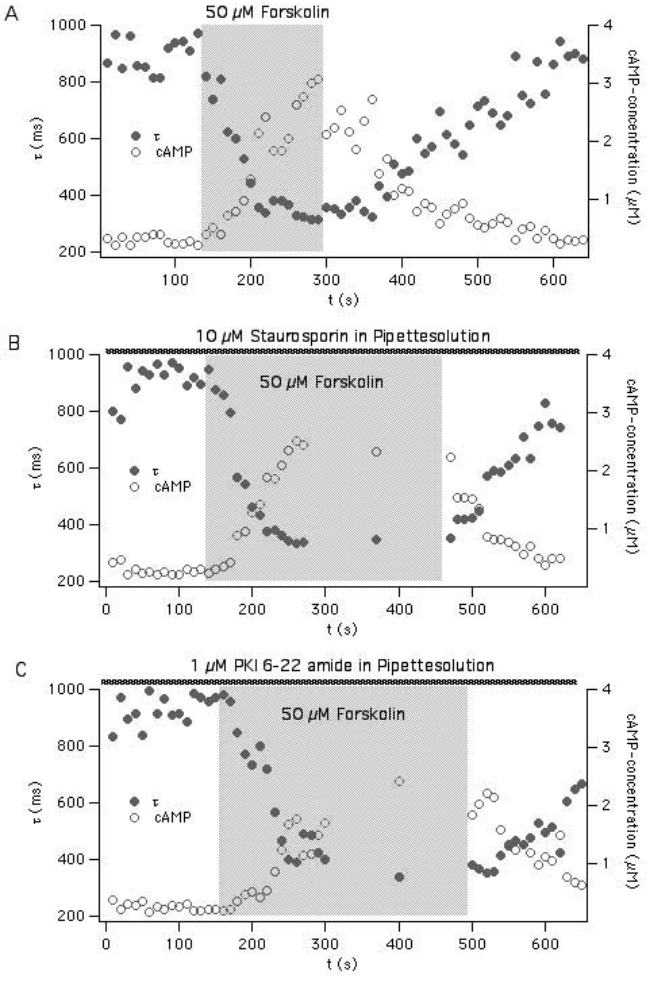

Fig. 3A–C Stimulation of Sf.9 cells expressing the recombinant HvCNG channel by 50 μM forskolin. **A** Time course of forskolin-induced decrease of τ_a fitted by single exponential functions and the calculated cAMP concentration are shown. The time to reach maximal activation was 87±5 s. τ_a was decreased from 730±79 ms to 353±45 ms (n=6). **B** Time course of forskolin-induced decrease of τ_a fitted by single exponentials in the presence of 10 μM staurosporine. The time to reach maximal activation was 157±23 s. τ_a was decreased from 749±117 ms to 465±76 ms (n=3). **C** Time course of forskolin-induced decrease of τ_a fitted by single exponentials in the presence of 1 μM PKI 6–22 amide. The time to reach maximal activation was 176±25 s. τ_a was decreased from 656±55 ms to 423±18 ms (n=5)

shift by maximally +28.5±1.7 mV (n=3), when cAMP varied between 0 μM and 100 μM (Fig. 2).

The activation time constants as measured at different cAMP concentrations were fitted by a Hill equation (Fig. 1C). We determined values of 0.62 μM for the half-maximal cAMP concentration (K_a) and 1.51 for the Hill coefficient (n). The K_a value was slightly lower than the K_a of 0.76 μM as reported elsewhere [14] using inside-out patches. However, the K_a determined in the present experiments is in good agreement with measurements made from other heterologously expressed HCN channels [8, 17, 28].

Changes of current kinetics through activation of endogenous adenylyl cyclases

Sf.9 cells have an endogenous steady-state level of intracellular cAMP. Experiments to measure this endogenous level of cAMP were performed on Sf.9 cells that were infected only by the HvCNG channel. The first –100 mV pulse immediately after establishing the whole-cell configuration was used to determine the basal cAMP level of the cells. We assumed a negligible degree of diffusion from the pipette into the cytosol after such a short time of about 10–20 s. The averaged mean τ_a value was 517±33 ms (n=49) and indicated a basal cAMP concentration of 1.5±0.3 μM. Incubation of cells in 30 μM MDL 12330A for at least 30 min shifted the τ_a value to 688±62 ms (n=15), which indicates a basal cAMP concentration of 0.9±0.1 μM. However, the τ_a values were not significantly different (unpaired t-test, P=0.097).

Application of 50 μM forskolin shifted the value for $V_{1/2}$ in the positive direction by +12.9±2.8 mV (n=3), while the τ_a value was reduced from 730±79 ms to 353±45 ms (n=6). The calculated τ_a corresponded with an increase of intracellular cAMP levels by 1.6±0.2 μM. The delay between drug application and maximal activation was found to be 87±5 s. Such activation of endogenous ACs was only partially reversible (Fig. 3A).

Involvement of protein kinases in channel activation

In order to verify that protein kinases do not modify the opening kinetics of HvCNG channels in addition to free cAMP, we applied two kinase antagonists. Staurosporine (10 µM) was used to block protein kinase C (PKC) as well as cAMP-dependent protein kinase (PKA). PKI 6–22 amide (1 µM) was applied to specifically block PKA. Neither antagonist had any influence on current kinetics when applied through the patch pipette or when applied extracellularly by local pressure ejection. The $V_{1/2}$ values did not change significantly and additional application of 50 µM forskolin affected the kinetics of the current in the same way as did forskolin application alone. The $V_{1/2}$ values induced by forskolin changed by about +10.6±1.3 mV (n=3) after staurosporine application and by about +11.5±1.3 mV (n=5) after the application of PKI 6–22 amide. Forskolin-induced (50 µM) modulation of τ_a changed from 749±117 ms to 465±76 ms (n=3) in the presence of 10 µM staurosporine, and from 656±55 to 423±18 ms (n=5) in the presence of 1 µM PKI 6–22 amide. The calculated increase of cAMP was 1.5±0.5 µM and 1.4±0.04 µM in the presence of staurosporine or PKI 6–22 amide, respectively, revealing that PKA inhibitors had no effect on the forskolin-induced increase of cAMP.

The only significant difference was seen in the delay of maximal activation of endogenous ACs that increased when PKA antagonists were applied. In the presence of 10 µM staurosporine the delay was 157±23 s (n=3) and with 1 µM PKI 6–22 amide it was 176±25 s (n=5) (Fig. 3B, C) as compared with 87±5 s during forskolin application alone.

Co-expression of HvCNG channels with the m5-$HT_{4(a)}$-receptor or the m5-HT_{1A}-receptor

Co-expression of HvCNG channels together with recombinant m5-$HT_{4(a)}$-receptors or m5-HT_{1A}-receptors and their G_s-proteins (α_s-, β_1-, γ_2-subunits) or G_i-proteins (α_{i2}-, β_1-, γ_2-subunits) affirmed that HvCNG channels can also be used as endogenous sensors for the intracellular cAMP changes that were induced by receptor activation. Expression of the m5-$HT_{4(a)}$-receptor and the m5-HT_{1A}-receptor together with heteromeric G_s-protein or G_i-protein was verified by Western blot analysis of the infected Sf.9 cells using appropriate antibodies (Fig. 4B).

In order to test whether serotonin (5-HT) is able to induce endogenous currents, we did several controls:

1. We applied 5-HT to Sf.9 cells that were infected only with m5-$HT_{4(a)}$-receptors (n=5, not shown) and also to Sf.9 cells co-expressing m5-$HT_{4(a)}$-receptors together with the G_s-proteins (α_s-, β_1-, γ_2-subunits) (n=4, Fig. 4A) both without the HvCNG channel.
2. We also tested cells that co-expressed HvCNG channels and m5-$HT_{4(a)}$-receptors without the G_s-protein (n=4, Fig. 4A).

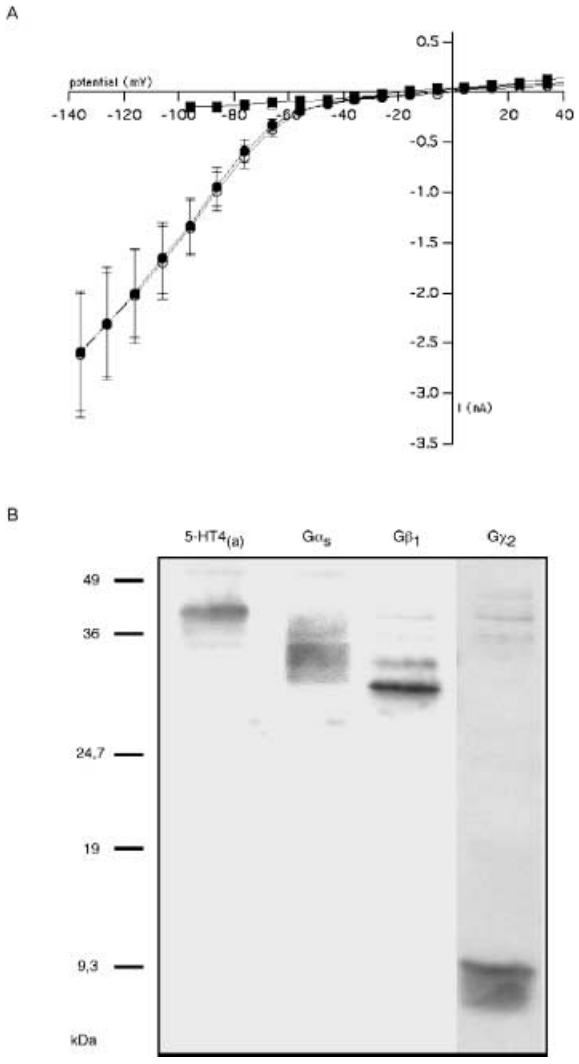

Fig. 4A, B Transfection with different baculoviruses encoding for HvCNG channel, 5-$HT_{4(a)}$-receptor and heterotrimeric G-protein subunits α_s, β_1 and γ_2. **A** Current–voltage (I–V) relationship showing no difference between currents recorded before (❑) and after (■) application of 100 µM 5-HT in cells that co-expressed the 5-$HT_{4(a)}$-receptor and the Gα_s-, Gβ_1- and Gγ_2-subunits without the HvCNG channel (n=4) or cells that co-express the HvCNG channel together with the 5-$HT_{4(a)}$-receptor (○/●), but without G-protein subunits (n=4). **B** Sf.9 cells infected with recombinant baculoviruses encoding for HvCNG channel, 5-$HT_{4(a)}$-receptor, Gα_s-, Gβ_1- and Gγ_2-subunits of heterotrimeric G-protein were harvested 48 h post-infection, washed with ice-cold PBS and resuspended in Tris/EDTA buffer. Probes were boiled in non-reducing electrophoresis sample buffer, separated on the 10% gel by the SDS-PAGE and then subjected to Western blotting with antibody AS9459 raised against the C-terminus of the 5-$HT_{4(a)}$-receptor, with antibodies against the Gα_s-subunit, with antibodies AS398 against β-subunits (β_1–β_4) and AS292 against the γ-subunits (γ_2+γ_3). In all cases polypeptide bands at the expected size were detected. The fluorogram shown is one of two independent experiments

In none of the tests did we observe any significant changes of currents during and after application of 100 µM 5-HT.

Responses to application of 5-HT were only seen in 10–15% of cells infected with viruses encoding for all

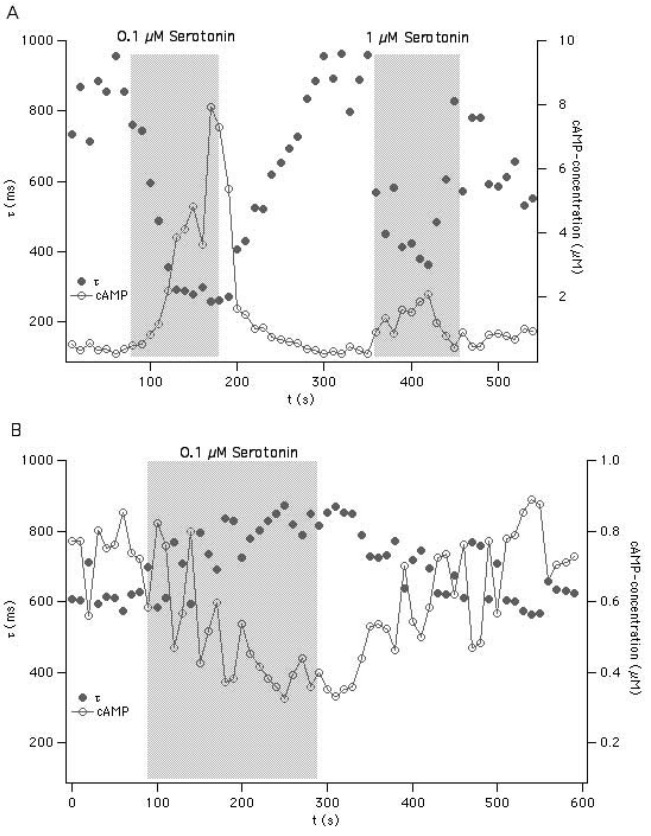

Fig. 5A, B Co-expression of recombinant m5-HT-receptors, G-protein subunits and the HvCNG channel in Sf.9 cells. **A** Stimulation by 0.1 µM 5-HT induced a pronounced decrease of τ_a of the evoked currents in Sf.9 cells expressing the m5-HT_{4a}-receptor, the G-protein-subunits α_s, β_1, γ_2 and the HvCNG channel. The time course shows a steep decrease of τ_a from 769±66 ms to 309±38 ms (*n*=6). The time to reach maximal activation was 70±4 s (*n*=6) for applications of 0.1 µM 5-HT. Repetitive stimulation of the m5-HT_{4a}-receptor revealed a strong reduction of the response to the second 5-HT application even at higher 5-HT concentrations. **B** Stimulation by 0.1 µM 5-HT induced an increase of τ_a in Sf.9 cells that had expressed the m5-HT_{1A}-receptor, the G-protein-subunits α_{i2}, β_1, γ_2 and the HvCNG channel. The time course shows a slow increase of τ_a from 545±57 ms to 805±41 ms (*n*=3). The time to reach maximal activation was 183±32 s (*n*=6) for applications of 0.1 µM 5-HT

three components, e.g. HvCNG channels, m5-$HT_{4(a)}$-receptors and G_s-proteins. These cells revealed maximal activation of HvCNG-channel-mediated currents 70±4 s (*n*=6) after exposure to 5-HT. τ_a decreased from 769±66 ms to 310±38 ms (4.6±1.45 µM cAMP) in response to 0.1 µM 5-HT, while τ_a increased again to 701±123 ms after wash-out (Fig. 5A). Repetitive applications of 5-HT induced a decline of responses (Fig. 5A). A tenfold elevation of the 5-HT concentration (1 µM) was not as effective at decreasing τ_a as compared with the first application of 0.1 M 5-HT. The decrease of the second response is clearly to be seen in the estimation of cAMP according to the dose–response curve in Fig. 1C. However, one has to be aware that the calculated cAMP levels during the first application correspond to τ_a values that are in the saturating range of the dose–response curve and may cause an overestimation of cAMP.

The τ_a values of some co-infected cells indicated that the intracellular cAMP level was elevated to 5 µM even under control conditions. This may indicate that over-expressed receptors reveal a basal activity that affects endogenous cAMP levels as described elsewhere [7]. On average, however, cAMP levels of 1.9±1.02 µM (τ_a=467±75; *n*=6) were not significantly different from the basal cAMP levels of 1.5±0.3 µM (τ_a=571±33; *n*=49) measured in Sf.9 cells that were only infected with the HvCNG channel.

Sf.9 cells, which were transfected with m5-HT_{1A}-receptor and G_i-protein (α_{i2}-, β_1-, γ_2-subunits), revealed an inhibitory response to 0.1 µM 5-HT (Fig. 5B). Application of 0.1 µM 5-HT decreased the cAMP level to 0.4±0.06 µM. τ_a increased from 545±57 ms to 805±41 ms, which returned to 662±32 ms after wash-out (*n*=3). The basal cAMP level was 1.5±0.3 µM (437±36 ms). The delay to reach stable current kinetics was 183±32 s.

The strong fluctuation of the τ_a values at the start of 5-HT application and during wash-out may reflect the activity of intracellular factors modulating the HvCNG channel activation kinetic, such as AC, PDE and protein phosphorylation, that we did not control in these experiments. However, especially for the estimation of cAMP we are in the linear range of the dose–response curve and have a highly sensitive tool for measuring even small changes of cAMP.

Discussion

In the present study we determine quantitatively the intracellular cAMP level and its change after pharmacological (forskolin, PKI, staurosporine) or molecular (m5-$HT_{4(a)}$-, m5-HT_{1A}-receptor, G_s-, G_i-protein) manipulations of intracellular signalling pathways. The recombinant HvCNG channel from the antennae of the moth *Heliothis virecens* was used as a sensor for intracellular cAMP. Several other ingenious methods have been developed [1, 29, 34] for performing a comparable quantification of the intracellular level of cyclic nucleotides. These methods are, however, very sophisticated and difficult to perform [29, 34]. They estimated that the cytosolic cyclic nucleotide concentration reaches maximally at 5 µM. Here we present a technique to estimate cAMP levels with HvCNG channels as biosensors, which have several advantages.

Advantages of the HvCNG channel

The HvCNG channel is favoured by its dual dependence on voltage and cAMP. CNG channels, which have been used in other investigations to determine the cAMP level [24, 29], monitor cAMP or cGMP levels as a function of current amplitudes. The limitation of this technique is

that the current amplitude depends on the expression level of the channel. Therefore, the use of CNG channels demands a difficult calibration of the level of CNG channel expression within each cell. The method described here is independent of the expression level because the measurements rely on the cAMP-induced kinetic shift in current activation as a direct parameter of the cAMP level. This allowed us to measure intracellular cAMP levels by the cAMP-dependent changes of the activation time constants independently from the expression level of HvCNG channels. Another advantage of the method is that the parameter is resistant to any wash-out effects during the period of whole-cell recordings. Electrodes containing defined concentrations of cAMP allowed accurate calibration. The parameter is also highly sensitive over a broad concentration range of 0.1–5 µM cAMP, which enables us to measure even small changes of the cAMP concentration.

Involvement of protein kinases in channel activation

To investigate whether cAMP acts directly on the HvCNG channel as reported for another HCN channel [8], we used staurosporine (10 µM) and PKI 6–22 amide (1 µM) to block any possible contributions of protein kinases, especially PKC and PKA. There was no effect on the forskolin-induced change of intracellular cAMP, but there was a significant increase in the rise time to reach maximal levels. This prolongation of the activation time was similar for the two antagonists and therefore may indicate the involvement of PKA in the process of HvCNG channel activation. Sequence analysis of the HvCNG channel has indeed demonstrated that there are ten putative phosphorylation sites for PKC and two phosphorylation sites for a tyrosine kinase [14]. HCN channels can be influenced by phosphorylation [6, 25, 30], which may play a role in the activation of the HvCNG channel. However, our investigations do support an action of PKA on the channel protein.

Forskolin-induced changes of the cAMP concentration indicate the existence of functional microdomains

As shown recently in C6–2B glioma cells and in HEK-293 cells, activation of ACs primarily induces a build-up of cAMP levels that are spatially restricted to microdomains, which is followed by a much slower increase of cAMP in the cytosol [24]. In their investigation Rich et al. [24] postulated a co-localization of olfactory CNG channels and ACs.

The Sf.9 cells have fairly weak endogenous currents [31] that may interfere with the expressed HvCNG channel (Fig. 4A). However, Sf.9-cells have the capacity to effectively produce measurable cAMP changes, as demonstrated by the forskolin-induced activation of ACs (Fig. 3). However, forskolin (50 µM) could not potentiate HvCNG channels as effectively as saturating concentrations (100 µM) of cAMP applied via the pipette solution. This became evident in the forskolin-induced (50 µM) shift of $V_{1/2}$ by +12.9 mV, which was much less than the +28.5-mV shift of $V_{1/2}$ obtained by perfusion of cAMP via the patch pipette. This indicates a restricted ability of the membrane-delimited ACs to elevate local cAMP levels and/or good efficiency of the endogenous PDEs. Inhibition of PDE activity by application of the unspecific antagonist IBMX did not influence the basal cAMP level or may not affect the endogenous PDEs (data not shown). However, endogenous PDEs are not effective below 0.9 µM intracellular cAMP, as indicated by the basal cAMP level measured in the presence of the AC antagonist MDL 12330A.

Krieger et al. [14] reported a Hill factor of 1 based on measurements of the HvCNG channel's responses in inside-out patches that were exposed to different cAMP concentrations. Such inside-out patches are not comparable with a whole-cell configuration. Thus, the Hill factor of 1.5, as revealed in our experiments, indicates that PDE activity is high (above 1 µM cAMP) and probably not present in inside-out patches.

The forskolin-induced effects on the current kinetics as observed under whole-cell conditions supports the results described elsewhere [24], namely that cAMP increases in microdomains with restricted diffusion into the cytosol. The lack of wash-out seen in the present experiments is also consistent with this view.

Receptor-induced changes of cAMP

There is no indication that endogenous ion channels contribute to the 5-HT-induced response of the co-expressed HvCNG channels (Fig. 4A). The observed changes of τ_a are only related to the expressed 5-HT receptors and G-protein subunits.

The time course of the 5-HT-induced cAMP increase is not significantly different from that of the cAMP changes induced by forskolin. This encourages us to argue that heterologously expressed components are aggregated in subcellular compartments; otherwise, one would expect longer time courses of changes in the current kinetics during 5-HT application because of longer diffusion distances.

Repetitive applications of 5-HT showed that the heterologously expressed 5-$HT_{4(a)}$-receptor desensitized after the first 5-HT application.

Another feature of the m5-$HT_{4(a)}$-receptor and different splice variants of the m5-HT_4-receptor is their high basal activity [7]. Following the hypothesis that the cAMP concentration in a subcellular domain around the AC is high and diffusion of cAMP out of this domain is impeded, we determined the basal activity in whole-cell recordings performed shortly after breakthrough of the membrane. In some cells we observed a higher basal activity that was not washed out even after a longer diffusion time, but the mean value was not significantly different from the basal activity measured in

Sf.9-cells, which were infected by the HvCNG channel alone.

To demonstrate that the Sf.9 expression system is valid for measuring an increase and a *decrease* of cAMP, we expressed the recombinant m5-HT_{1A}-receptor together with G_i-protein (α_{i2}-, β_1-, γ_2-subunits). We observed a reversible increase of τ_a and therefore a decrease of cAMP in response to 0.1 µM 5-HT (Fig. 5). We assume that the slow time course of the cAMP decline indicates a slow rate of cAMP degradation or diffusion. As suggested by the Hill factor, there is efficient PDE-regulated degradation of higher cAMP levels that determines the decline of cAMP levels after the AC activity is decreased by the α_i-subunit. Several processes might interact to bring about the long degradation time of cAMP after m5-HT_{1A}-receptor stimulation. Firstly, PDE may not be efficient enough to change the cAMP concentration in a shorter time in this concentration range, as indicated by the basal cAMP level measured after prolonged blockade of endogenous ACs by MDL 12330A. Secondly, there is indication of a diffusional process out of the microdomain, with impeded diffusion into the cytosol [24].

We measured membrane-delimited cAMP levels at the effectors that are regulated by cAMP. This should be used as a tool for obtaining valuable information about the molecular machinery of intracellular signalling within the microenvironment of cAMP target structures.

Acknowledgements We thank Professor Dr. H. Breer for providing the recombinant HvCNG/AcNMPV baculovirus, Dr. M. Haller and Dr. U. Markstahler for fruitful discussions. Deutsche Forschungsgemeinschaft grants SFB 406, medical school of Göttingen and the graduate school: "Organization and Dynamic of neuronal networks" supported the work.

References

1. Adams SR, Harootunian AT, Beuchler YJ, Taylor SS, Tsien RY (1991) Fluorescence ratio imaging of cyclic AMP in single cells. Nature 349:694–697
2. Albert PR, Sajedi N, Lemonde S, Ghahremani MH (1999) Constitutive G(i2)-dependent activation of adenylyl cyclase type II by the 5-HT1A receptor. Inhibition by anxiolytic partial agonists. J Biol Chem 274:35469–35474
3. Barnes NM, Sharp T (1999) A review of central 5-HT receptors and their function. Neuropharmacology 38:1038–1152
4. Budde T, Biella G, Munsch T, Pape H-C (1997) Lack of regulation by intracellular Ca^{2+} of the hyperpolarization-activated cation current in rat thalamic neurons. J Physiol (Lond) 503: 79–85
5. Cathala L, Paupardin-Tritsch D (1999) Effect of catecholamines on the hyperpolarization-activated cationic I_h and the inwardly rectifying potassium I_{kir} currents in the substantia nigra pars compacta. Eur J Neurosci 11:398–406
6. Chang F, Cohen IS, Di Francesco D, Rosen MR, Tromba C (1991) Effects of protein kinase inhibitors on canine purkinje fiber pacemaker depolarization and the pacemaker current $i_{(f)}$. J Physiol (Lond) 440:367–384
7. Claeysen S, Sebben M, Becamel C, Bockaert J, Dumuis A (1999) Novel brain-specific 5-HT_4 receptor splice variants show marked constitutive activity: role of the C-terminal intracellular domain. Mol Pharmacol 55:910–920
8. DiFrancesco D, Tortora P (1991) Direct activation of cardiac pacemaker channels by intracellular cyclic AMP. Nature 351:145–147
9. Dumuis AR, Bouhelal M, Sebben RC, Bockaert A (1988) A non-classical 5-hydroxytryptamine receptor positively coupled with adenylate cyclase in central nervous system. Mol Pharmacol 34:880–887
10. Finn JT, Grunwald ME, Yau K-W (1996) Cyclic nucleotide-gated ion channels: an extended family with diverse functions. Annu Rev Physiol 58:395–426
11. Gasparini S, DiFrancesco D (1999) Action of serotonin on the hyperpolarization-activated current (Ih) in rat CA1 hippocampal neurons. Eur J Neurosci 11:3093–3100
12. Gudermann T, Kalkbrenner F, Schultz G (1996) Diversity and selectivity of receptor-G protein interaction. Annu Rev Pharmacol Toxicol 36:429–459
13. Guellaen G, Mahu JL, Mavier P, Berthelot P, Hanoune J (1977) RMI 12330A, an inhibitor of adenylate cyclase in rat liver. Biochim Biophys Acta 13:465–475
14. Krieger J, Strobel J, Vogl A, Hanke W, Breer H (1999) Identification of a cyclic nucleotide- and voltage-activated ion channel from insect antennae. Insect Biochem Mol Biol 29: 255–267
15. Leopoldt D, Harteneck C, Nurnberg B (1997) G proteins endogenously expressed in Sf.9 cells: interactions with mammalian histamine receptors. Naunyn Schmiedebergs Arch Pharmacol 356:216–224
16. Liu YF, Ghahremani MH, Rasenick MM, Jakobs KH, Albert PR (1999) Stimulation of cAMP synthesis by Gi-coupled receptors upon ablation of distinct Galphai protein expression. Gi subtype specificity of the 5-HT1A receptor. J Biol Chem 274:16444–16450
17. Ludwig A, Zong X, Jeglitsch M, Hofman F, Biel M (1998) A family of hyperpolarization-activated mammalian cation channels. Nature 393:587–591
18. Lüthi A, McCormick DA (1998) Periodicity of thalamic synchronized oscillations: the role of Ca^{2+}-mediated upregulation of Ih. Neuron 20:553–563
19. Neer EJ (1995) Heterotrimeric G proteins: organizer of transmembrane signals. Cell 80:249–257
20. Neher E (1992) Correction for liquid junction potentials in patch clamp experiments. Methods Enzymol 207:123–131
21. Pape H-C (1996) Queer current and pacemaker: the hyperpolarisation-activated cation current in neurons. Annu Rev Physiol 58:299–327
22. Pape H-C, McCormick DA (1989) Noradrenaline and serotonin selectively modulate thalamic burst firing by enhancing a hyperpolarization-activated cation current. Nature 340: 715–718
23. Ponimaskin EG, Schmidt MFG, Heine M, Bickmeyer U, Richter DW (2001) 5-Hydroxytryptamine(4a) receptor expressed in Sf.9 cells is palmitylated in an agonist-dependent manner. J Biochem 353:627–634
24. Rich TC, Fagan KA, Nakata H, Schaack J, Cooper DM, Karpen JW (2000) Cyclic nucleotide-gated channels colocalize with adenylyl cyclase in regions of restricted cAMP diffusion. J Gen Physiol 116:147–162
25. Ruiz ML, Brown RL, He Y, Haley TL, Karpen JW (1999) The single-channel dose-response relation is consistently steep for rod cyclic nucleotide-gated channels: implications for the interpretation of macroscopic dose–response relations. Biochemistry 38:10642–10648
26. Sambrook J, Fritsch EF, Maniatis T (1989) Molecular cloning: a laboratory manual. Cold Spring Harbor Laboratory Press, New York
27. Santoro B, Tibbs GR (1999) The HCN gene family: molecular basis of the hyperpolarization-activated pacemaker channels. Ann NY Acad Sci 868:741–764
28. Santoro B, Chen S, Lüthi A, Pavlidis P, Shumyatsky GP, Tibbs GR, Siegelbaum SA (2000) Molecular and functional heterogeneity of hyperpolarization-activated pacemaker channels in the mouse. J Neurosci 20:5264–5275
29. Trivedi B, Kramer RH (1998) Real-time patch-cram detection of intracellular cGNP reveals long-term suppression of responses to NO and muscarinic agonists. Neuron 21:895–906

30. Vargas G, Yeh T-YJ, Blumenthal DK, Lucero MT (1999) Common components of patch-clamp internal recording solutions can significantly affect protein kinase A activity. Brain Res 828:169–173
31. Vasudevan S, Premkumar L, Stowe S, Gage PW, Reilander H, Chung S-H (1992) Muscarinic acethylcholine receptor produced in recombinant baculovirus infected Sf9 insect cells couples with endogenous G-proteins to activate ion channels. FEBS Lett 311:7–11
32. Veit M, Nürnberg B, Spicher K, Harteneck C, Ponimaskin E, Schultz G, Schmidt MFG (1994) The alpha-subunits of G proteins G12 and G13 are palmitoylated, but not amidically myristoylated. FEBS Lett 339:160–164
33. Wei J-Y, Roy DS, Leconte L, Barnstable CJ (1998) Molecular and pharmacological analysis of cyclic nucleotide-gated function in the central nervous system. Prog Neurobiol 56:37–64
34. Zaccolo M, De Giorgi F, Cho CY, Feng L, Knapp T, Negulescu PA, Taylor SS, Tsien RY, Pozzan T (2000) A genetically encoded, fluorescent indicator for cyclic AMP in living cells. Nature Cell Biol 2:25–29
35. Zagotta WN, Siegelbaum SA (1996) Structure and function of cyclic nucleotide-gated channels. Annu Rev Neurosci 19: 235–263